# Contribution of Electric Field ($\Delta\psi$) to Steady-State Transthylakoid Proton Motive Force (*pmf*) in Vitro and in Vivo. Control of *pmf* Parsing into $\Delta\psi$ and ΔpH by Ionic Strength†

Jeffrey A. Cruz, Colette A. Sacksteder, Atsuko Kanazawa, and David M. Kramer*

*Institute of Biological Chemistry, Washington State University, Pullman, Washington 99164-6340*

*Received August 9, 2000; Revised Manuscript Received December 7, 2000*

ABSTRACT: The observed levels of $\Delta G_{ATP}$ in chloroplasts, as well as the activation behavior of the $CF_1CF_0$-ATP synthase, suggest a minimum transthylakoid proton motive force (*pmf*) equivalent to a ΔpH of ∼2.5 units. If, as is commonly believed, all transthylakoid *pmf* is stored as ΔpH, this would indicate a lumen pH of less than ∼5. In contrast, we have presented evidence that the pH of the thylakoid lumen does not drop below pH ∼5.8 [Kramer, D. M., Sacksteder, C. A., and Cruz, J. A. (1999) *Photosynth. Res. 60*, 151−163], leading us to propose that $\Delta\psi$ can contribute to steady-state *pmf*. In this work, it is demonstrated, through assays on isolated thylakoids and computer simulations, that thylakoids can store a substantial fraction of *pmf* as $\Delta\psi$, provided that the activities of ions permeable to the thylakoid membrane in the chloroplast stromal compartment are relatively low and the buffering capacity ($\beta$) for protons of the lumen is relatively high. Measurements of the light-induced electrochromic shift (ECS) confirm the ionic strength behavior of steady-state $\Delta\psi$ in isolated, partially uncoupled thylakoids. Measurements of the ECS in intact plants illuminated for 65 s were consistent with low concentrations of permeable ions and ∼50% storage of *pmf* as $\Delta\psi$. We propose that the plant cell, possibly at the level of the inner chloroplast envelope, can control the parsing of *pmf* into $\Delta\psi$ and ΔpH by regulating the ionic strength and balance of the chloroplast. In addition, this work demonstrates that, under certain conditions, the kinetics of the light-induced ECS can be used to estimate the fractions of *pmf* stored as $\Delta\psi$ and ΔpH both in vitro and in vivo.

In the chemiosmotic mechanism proposed by Mitchell (*1*), free energy released from exergonic reactions (metabolism or the electron transfer reactions of photosynthesis) is stored in the form of a transmembrane electrochemical gradient of protons, called the proton motive force (*pmf*).[1] In turn, the dissipation of *pmf* is coupled to the synthesis of ATP. Because protons are charged, *pmf* consists of two components, i.e., transmembrane differences in the concentration of protons (expressed as ΔpH) and in the electric field ($\Delta\psi$). It has been established that the two components of *pmf* are thermodynamically equivalent (*2*), so the total driving force for ATP synthesis may be expressed as the sum of these energetic components:

$$pmf = \Delta\psi_{i-o} + \frac{2.3RT}{F}\Delta pH_{o-i} \qquad (1)$$

where $\Delta\psi_{i-o}$ and $\Delta pH_{o-i}$ represent the electric field and the difference in pH, respectively, calculated as outside (stroma) minus inside (lumen), $R$ is the universal gas constant, and $F$ is Faraday's constant. Conversely, in thermodynamic terms, *pmf* may be parsed equivalently into $\Delta\psi$ and ΔpH.

The kinetic and physiological consequences of storing *pmf* in these two forms are clearly different. First, $\Delta\psi$ and ΔpH are not kinetically equivalent driving forces at the ATP synthase. In the cases of the mitochondrial and *Escherichia coli* enzymes, $\Delta\psi$ is the more effective component of *pmf* for maintaining catalytic turnover, while for the chloroplast enzyme, $\Delta\psi$ and ΔpH are nearly equivalent (*3*−*6*). Thus, it has been argued that some $\Delta\psi$ is required, at least for respiration (*7*). Physiologically, the establishment of a substantial ΔpH component in mitochondria and bacteria would incur a substantial alteration of pH in one or more cellular compartments. Consequently, these systems possess molecular machinery for maintaining *pmf* predominantly in

† This work was supported by U.S. Department of Energy Grant DE-FG03-98ER20299.

* To whom correspondence should be addressed: Institute of Biological Chemistry, Washington State University, Pullman, WA 11964-6340. Telephone: (509) 335-4964. Fax: (509) 335-7643. E-mail: dkramer@wsu.edu.

[1] Abbreviations: ATP synthase, $(C)F_1$-$(C)F_0$-ATP synthase; $\beta$, buffering capacity; $c_i$, concentration of ion i at the thylakoid membrane; CPC, compound parabolic concentrator; cyt, cytochrome; $\Delta\psi$, electrical component of the proton motive force; ΔpH, osmotic component of the proton motive force; $\Delta\tilde{\mu}_i$, difference in chemical activities of ion i; DOFS, diffused optics flash spectrophotometer; ECS, electrochromic shift of light-harvesting pigments; $ECS_{ss}$, extent of ECS signal in the steady state; $ECS_{inv}$, change in ECS upon a rapid light−dark transition, which extends below the baseline taken in the dark and reflecting the diffusion potential of ΔpH; $ECS_t$, total difference in ECS signals upon shuttering the actinic light ($EVS_{ss} - EVS_{inv}$), reflecting the total steady-state *pmf*; EDTA, ethylenediaminetetraacetic acid; CCCP, carbonyl *m*-(chlorophenyl)hydrazone; $g_{H^+}$, conductivity of protons across the thylakoid membrane; HEPES, *N*-(2-hydroxyethyl)piperazine-*N*′-2-ethanesulfonic acid; *I*, ionic strength; LHC, light-harvesting complex; $\phi_{H^+}$, flux of protons across the thylakoid membrane; $\phi_i$, flux of ion i across the thylakoid membrane in moles per liter per second; *pmf*, proton motive force.

10.1021/bi0018741 CCC: $20.00 
Published on Web 01/30/2001

the form of $\Delta\psi$ so as to prevent inactivation of important acid-label enzymes (e.g., refs *8* and *9*).

In contrast, despite early work showing that *pmf* can be stored as $\Delta\psi$ as long as the concentrations of permeable ions are low (*10*−*13*), it has become the textbook view that thylakoids of higher plants store *pmf* almost exclusively as $\Delta$pH (see refs *14*−*17*). This conclusion was mainly derived from work on isolated thylakoid membranes and on giant chloroplasts of *Peperomia metallia* (see review in ref *17*). Upon illumination, several phases of *pmf* storage are observed in these experimental systems. The electrical capacitance of the thylakoid membrane is relatively low, $\sim$0.6−1 $\mu$F/cm$^2$, but the proton buffering capacities of the lumen and stroma are high (*18*, *19*). Consequently, when actinic light is applied, *pmf* is first formed almost exclusively as $\Delta\psi$. However, $\Delta\psi$ collapses on the time scale of many seconds as counterions, notably, $Cl^-$, $Mg^{2+}$, and $K^+$, leak across the thylakoid membrane in response to the electric field (*17*, *18*, *20*, *21*). Essentially, $\Delta\psi$ is replaced by ion gradients. If the overall ionic strengths of thylakoid membrane permeable ions (*I*) are high, the resulting transmembrane ratios of ion concentrations will be small, and the majority of $\Delta\psi$ will be dissipated.

Indeed, it can be argued that a pH homeostatic apparatus in thylakoids is superfluous, and thus would have been lost during evolution, because relatively few enzymes are contained in the lumen, and that these may have evolved to tolerate low pH. On the other hand, we have recently presented arguments, based on the enzymatic properties and stabilities of lumenal enzymes, that the pH of the thylakoid lumen does not drop below 5.8 during normal in vivo photosynthesis (*22*). A similar conclusion was reached by Tikhonov and co-workers based on $\Delta$pH estimates and $P_{700}^+$ re-reduction kinetics (*23*, *24*). To reconcile such a moderate lumen pH with the requirement for >120 mV in *pmf*, we suggested that $\Delta\psi$ may contribute significantly to *pmf*, at least under some conditions (*22*).

There is, in fact, some evidence in the literature to support a long-lived $\Delta\psi$ component of *pmf*, at least under special circumstances. On the basis of the contributions of electrochromic shifts (ECSs) of light-harvesting pigments with quadratic and linear dependencies on $\Delta\psi$, Joliot and Joliot (*25*) and Finazzi and Rappaport (*26*) have argued that a stable $\Delta\psi$ is held across the thylakoid membrane of green algae *Chlamydomonas reinhardtii* and *Chlorella sorokiniana* in the dark. We have shown that a light-induced transthylakoid $\Delta\psi$ is held during a 40 s illumination in intact higher plant leaves (*27*), but the magnitude of this field has been difficult to assess (see the discussion in refs *28* and *29*).

The transthylakoid proton gradient is not only the energetic intermediate for ATP synthesis but also a key feedback regulatory component for controlling the photosynthetic apparatus (reviewed in ref *22*). In chloroplasts, light is captured by a set of light-harvesting complexes (LHCs) that funnel energy into reaction centers, photosystem I (PS I) and photosystem II (PS II). The absorbed energy drives the transfer of electrons through a series of redox carriers called the electron transfer chain (ETC). Ultimately, the electron path leads from the oxygen-evolving complex of PS II (which oxidizes $H_2O$ and releases $O_2$) and continues through the cytochrome (cyt) $b_6f$ complex to PS I, which transfers electrons to ferredoxin, which in turn reduces $NADP^+$ to NADPH. Electron flux is coupled to the "pumping" of protons across the thylakoid membrane, thereby establishing an electrochemical potential of protons that drives the synthesis of ATP by a chemiosmotic circuit. In this manner, the energy-storing substrates ATP and NADPH are formed for later use by the Calvin−Benson cycle and other biochemical processes.

The photosynthetic apparatus must be well-regulated to prevent overexcitation of the photosystems, which can lead to photoinhibition (or photodestruction) of the photosynthetic machinery (see the review in ref *30*). There is strong evidence that photoinhibition can result from hindering the reactions of the OEC, leading to the formation of highly oxidizing and reactive species (*31*). This "donor side" photoinhibition is exacerbated by low lumen pH that results from proton pumping (*32*, *33*). Alternatively, over-reduction of the ETC may also lead to "acceptor side" inhibition at two separate points. If $Q_A$, the primary quinone acceptor of PS II, becomes over-reduced, it forms a stable plastoquinol ($PQH_2$), which cannot accept further electrons. PS II centers blocked in this way tend to produce chlorophyll triplet states, which can interact with atmospheric $O_2$ to form the toxic singlet oxygen ($^1O_2$). There is also good evidence that over-reduction can permanently damage the PS I reaction center, perhaps at the level of the iron−sulfur centers, and especially at low temperatures (*34*−*39*).

It seems clear that either electron transfer or proton pumping in excess of the biochemical demands for NADPH or ATP, respectively, can lead to photoinhibition. Over the time scale of minutes to hours, photoinhibition is prevented in vivo by two main downregulatory processes that limit the number of photons reaching the PS II reaction centers (see reviews in refs *40*−*42*): the xanthophyll cycle and membrane energization-activated nonphotochemical quenching (NPQ) of antenna excitons (or $q_E$). Both of these processes are activated by acidification of the lumen (e.g., refs *40*, *43*, and *44*). In turn, these processes protect the photosynthetic apparatus from overexcitation by harmlessly converting large fractions of absorbed energy into heat. At full sunlight, a limited capacity for assimilatory processes, coupled to these downregulatory processes, can result in more than 90% of the absorbed light being shunted to heat. As far was we now know, the only rapidly responding photoprotective process controlled by the ETC redox state is the so-called "state transition", which probably accounts for a relatively small level of photoprotection (*45*, and references therein).

Given the importance of *pmf* and lumen pH in the photosynthetic energy budget, we considered the possibility that the in vivo storage of *pmf* may differ from that observed in vitro or in electrode-impaled cells, where ionic balance may be disrupted. New instrumentation developed in our laboratory (*27*) has made possible analysis of steady-state changes in the electrochromic shifts (ECS) of light-harvesting pigments, which linearly reflect the transthylakoid electric field (*46*, *47*). In this paper, we present data using this tool, indicating that a substantial fraction of *pmf* can be stored as $\Delta\psi$ indefinitely under continuous light, as long as the ionic strength of the stroma is low and the buffering capacity ($\beta$) of the lumen for protons is high. Computer simulations also indicate that the fractions of *pmf* stored as $\Delta\psi$ and $\Delta$pH under steady-state conditions can be estimated by analyzing the decay kinetics of the ECS, which is linear with $\Delta\psi$ (*46*),

upon shuttering the actinic light, possibly allowing their assay in vivo. We argue that changes in the parsing of *pmf* into $\Delta\psi$ and $\Delta$pH will have a substantial effect on the regulatory behavior of the chloroplast and propose a homeostatic mechanism wherein the *pmf* parsing could be adjusted to match the regulatory sensitivity to environmental conditions.

## EXPERIMENTAL PROCEDURES

*Computer Simulations*. Computer simulations were performed on a personal computer using a program written in-house in Microsoft Visual Basic 6.0. The algorithm assumed that, for brief time periods ($10^{-4}$ s), flux through each step was linearly related to either Ohm's law or the flux equation (see below). Simulations performed with time periods that differed by a factor of 2 gave essentially identical results, indicating that our "Newtonian approximation" was valid. Details of the model are presented in the next section.

*Working Model for Simulations of Steady-State pmf. (1) The Light Reactions.* The photosynthetic electron transfer reactions were simplified by treating them as a single, light-driven proton-pumping step. Because high concentrations of methyl viologen (MV) were added to the thylakoid suspensions (see below), electron transfer was probably never limited by the PS I electron acceptor. Acidification of the lumen can significantly hinder electron transfer in isolated thylakoids by slowing $PQH_2$ oxidation (*48*, *49*, and references therein). With this in mind, we incorporated the observed pH dependence of plastoquinol ($PQH_2$) oxidation, as discussed in ref *22*, using the approximation that a single p$K_a$ at pH 5.5 controlled cytochrome $b_6f$ activity. The maximal turnover of the cyt $b_6f$ complex was set to 100 $s^{-1}$ at pH 8 (*23*, *50*−*55*), and activity dropped in proportion to degree of protonation of the putative control group. Of course, electron transfer will be slowed by the buildup of both forms of *pmf*, but $\Delta\psi$ exerts significantly less control (*26*). For the present (simplified) simulations, control by $\Delta\psi$ was ignored. Three protons were pumped into the lumen per electron transferred to the stroma under all conditions (*56*, and references therein).

*(2) Passive Counterion Fluxes*. Counterion movements were modeled using an equation described in the pioneering work of Vredenberg and co-workers (*14*, *15*, *18*, *57*), but modified to account for both osmotic and electric driving forces for ion movements. This is critical for simulation of the steady state since the osmotic and electric potentials will come into equilibrium. The flux of an ion, $\phi_i$, is described by

$$\phi_i = P_i c_i \Delta\tilde{\mu}_i \tag{2}$$

where $P_i$ is the permeability of the ion through the membrane, $c_i$ is the concentration of the ion at the membrane, and $\Delta\tilde{\mu}_i$ is the difference in the chemical activities of permeable ions on the two sides of the membrane, defined for each by

$$\frac{\Delta\mu_i}{F} = z\Delta\psi_{i-o} + \frac{2.3RT}{F}\log\left(\frac{[i]_i}{[i]_o}\right) \tag{3}$$

where $z$ is the charge of the ion, $\Delta\psi_{i-o}$ is the membrane potential, $F$ is Faraday's constant, and $[i]_i$ and $[i]_o$ are ion concentrations in the lumen and stromal compartments, respectively. This treatment assumed that, for small concentration differences, osmotic and electric field driving forces were equivalent and that the ion channels were not activated by membrane potential or pH. As discussed below, this is only an approximation of the, sometimes, complex behavior of the channels. The values of $P_{Cl^-}$, $P_{K^+}$ were taken from the literature to be $1.8 \times 10^{-8}$ and $3.6 \times 10^{-8}$ cm $s^{-1}$ (reviewed in ref *58*). Recently, the permeability of $Mg^{2+}$ through thylakoid cation channels was found to be similar to that of $K^+$ (*59*), and thus, we set $P_{Mg^{2+}} = P_{K^+}$.

*(3) Turnover of the ATP Synthase*. The kinetics of proton transfer through the intact ATP synthase are dependent in a complex way on the *pmf*, since it both activates the enzyme and drives the reaction (*29*, *60*, *61*). In our in vitro studies, we simplified the problem by partially uncoupling the thylakoids in two ways: by addition of limiting amounts of carbonyl *m*-(chlorophenyl)hydrazone (CCCP) and by partial depletion of $F_1$ subunits from the ATP synthase (see below). This allowed us to approximate the rapid flux of protons observed in vivo without the addition of ADP and $P_i$, and to ignore much of the complexity of ATP synthase activation processes. Under these conditions, we assume that proton flux follows Ohm's law:

$$\phi_{H^+} = pmf \times g_{H^+} \tag{4}$$

where $\phi_{H^+}$ is the flux of protons across the membrane and $g_{H^+}$ is the conductivity of protons through the membrane. Changes in $g_{H^+}$ in our simulations by 2 orders of magnitude affected the amplitude of *pmf*, but did not significantly affect the parsing of *pmf* into $\Delta\psi$ and $\Delta$pH (see below). We concluded that this level of accuracy would suffice for the purposes of this work, and the more subtle consequences of non-Ohmic proton conductivity will be addressed in a more detailed model to follow. On the basis of previous work (*6*, *62*), assuming that $n$, the ratio of $H^+$ to ATP, was 4 and that there were $10^{-13}$ mol of ATP synthase $cm^{-2}$ (see below), we arrive at a value for $g_{H^+}$ of $1 \times 10^{-9}$ mol of $H^+$ $cm^{-2}$ $V^{-1}$ $s^{-1}$.

*(4) Chloroplast Proton Buffering Capacity*. For our simplified calculations, the pH of the stroma was assumed to be constant in the light at about 7.6. This was certainly true in our thylakoid experiments, and consistent with previous in vivo observations (*63*, *64*). On the other hand, the buffering capacity of the lumen is important for understanding the partitioning of *pmf* into $\Delta\psi$ and $\Delta$pH (see below). The buffering capacity is derived from expansion of the simple equilibrium equation

$$K_i = \frac{[H^+][B_i^-]}{[B_iH]} \tag{5}$$

where $K_i$ is the association constant for proton binding to buffering group $B_i^-$. When the concentrations of buffering groups are evenly distributed over the pH range of interest, a linear relationship between the total proton concentration and pH is observed (see refs *19* and *65*), where $\beta$, the buffering capacity, is defined as

$$\beta \equiv \frac{d([H_f^+] + \sum_{i=1}^{n}[B_iH])}{d(pH)} \tag{6}$$

The concentrations of buffering pools reviewed in ref *66* yield a range of $\beta$ from 0.02 to 0.08 M/pH. We used a value for $\beta$ of 0.03 M/pH, in agreement with the value obtained by Junge and co-workers (*19*), because it gave the best fit to our experimental data (see below).

*(5) Other Thylakoid Properties*. Other relevant properties of the thylakoid system were taken from the literature as follows. The membrane capacitance was taken to be 0.6 $\mu$F/cm$^2$, while the ratio of lumen volume to thylakoid surface area was taken to be 0.8 nL/cm$^2$ (reviewed in refs *18* and *58*). No light-induced changes in lumen volume were allowed, though these may be important considerations for future work (see below). On the basis of electron micrographic analysis (*67*), we estimated that there were approximately $2 \times 10^{-13}$ mol of PSI and PSII cm$^{-2}$ and $10^{-13}$ mol of ATP synthase cm$^{-2}$ with respect to the thylakoid membrane area. These values were similar to those used by Vredenberg and co-workers (*17*, *58*). Stroma and lumen ion and proton concentrations were assumed to be equal before illumination (i.e., no basal or dark ion gradients or *pmf*).

*Plant Material and Thylakoid Isolation.* Spinach plants were grown in a greenhouse as described in ref *68*. Freshly isolated thylakoids were obtained from market- or greenhouse-grown spinach as described in ref *69* except that they were resuspended in low-salt buffer containing 5 mM *N*-(2-hydroxyethyl)piperazine-*N*′-2-ethanesulfonic acid (HEPES)/NaOH (pH 7.6) and 330 mM sorbitol and used immediately. In some cases, partial depletion of the $CF_1$ portion of the ATP synthase was achieved by a procedure adapted from that described by Engelbrecht et al. (*70*), in which thylakoids were incubated ($\sim$14 $\mu$g of chlorophyll/mL) in buffer containing 20 $\mu$M EDTA, 5 mM HEPES/NaOH (pH 7.6), and 330 mM sorbitol for 30 min in darkness on ice. The extent of $F_1$ depletion was adjusted so that the resulting decay of the ECS upon shuttering the actinic light was approximately that observed in vivo (see below). After the $CF_1$ depletion, thylakoids were pelleted at 10000*g* for 10 min and resuspended in low-salt buffer.

For assays of the ECS, thylakoids were diluted to 20 $\mu$g of chlorophyll/mL in low-salt buffer containing 1 mM MV, as a photosystem I acceptor. Where noted, KCl or $MgCl_2$ was added from an aqueous 2.5 M stock. The dichloride salt of methyl viologen, sorbitol, and HEPES were purchased from Sigma Chemical Corp. All other chemicals were reagent grade.

*Kinetic Spectroscopy*. Light-induced kinetics of the ECS in leaves were obtained using a diffused optics flash spectrophotometer (DOFS), designed to reduce interference from light-induced light scattering (*27*). For thylakoid studies, a modified DOFS instrument was constructed to allow use of standard glass cuvettes. The measuring beam exiting the diffused optics beam splitter was partially collimated by a compound parabolic concentrator (CPC) (*71*) and passed through the reference and experimental samples and blocking filters. Light exiting the samples was concentrated using a second set of CPCs and directed into the photodiode detectors. This optical setup allowed the use of 1 cm path length, 1.5 cm diameter cylindrical cuvettes, while maintaining the reduced sensitivity to light scattering changes of the DOFS instrument. The actinic light was provided by a ring of seven red light-emitting diodes with maximal emission at 644 nm (HLMP C116), providing approximately 300 $\mu$mol of photons m$^{-2}$ s$^{-1}$ along the measuring beam axis. The optical axis of the instrument was vertical, reducing the effects of sample settling on long time span measurements to <100 ppm/min. This was a crucial feature for this work, where typical traces spanned several minutes. A more detailed description of the instrument will be presented elsewhere.

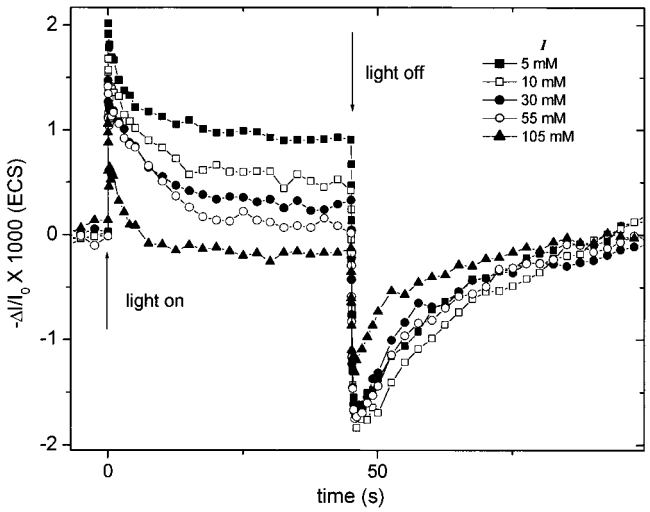


FIGURE 1: Effects of ionic strength on continuous light-induced changes in electrochromic shift (ECS) in isolated spinach thylakoids. Thylakoids (10 $\mu$g of chlorophyll/mL) were suspended in low-ionic strength resuspension buffer with added KCl. The ECS was measured as described in Experimental Procedures. At time zero, samples were illuminated with 300 $\mu$mol of photons of of red light m$^{-2}$ s$^{-1}$ for 45 s. The estimated ionic strengths, *I*, were 5 (■), 10 (□), 30 (●), 55 (○), and 105 mM (▲).

*Deconvolution of the ECS from Light Scattering Changes*. Changes in the light scattering properties of our sample are expected when the shapes of the thylakoids or chloroplasts change, particularly when the osmotic balance between the stroma and lumen is altered during illumination. This should occur when the lumen pH changes, i.e., when significant changes occur in the osmotic component of *pmf* (e.g., refs *72*−*77*). The spectrum of the scattering changes will depend on the optical properties of the sample (*78*) as well as the instrument (*27*) and thus must be determined in situ. The spectral contributions of the ECS and light scattering for leaves were obtained as described in ref *27*. For thylakoids, these contributions were obtained by treating samples with 50 mM KCl and 10 $\mu$M nonactin (Sigma Chemical Corp.) to suppress the ECS. A component spectrum for the ECS in thylakoids was obtained by illuminating thylakoids in low salt concentrations and in the absence of nonactin for brief (<1 s) periods that allowed buildup of $\Delta\psi$ but not $\Delta$pH (see the discussion in ref *27*). The spectra (not shown) were very similar to those reported for leaves (*27*). Several deconvolution procedures, including the two-wavelength procedure given in ref *27*, yielded similar results, but the most reliable was obtained by subtracting a baseline, taken between signals at 505 and 535 nm, from that at 515 nm, essentially eliminating the scattering component but retaining a large fraction of the ECS.

## RESULTS

*Effects of Ionic Strength on Partitioning of Transthylakoid pmf into $\Delta\psi$ and $\Delta$pH.* Figures 1 and 2 show the effects of

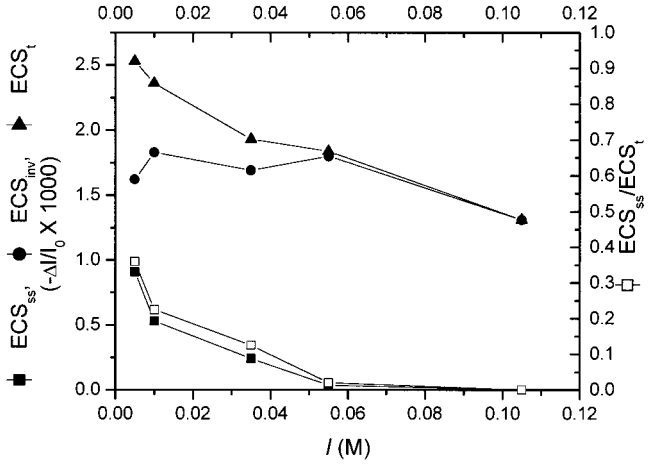


FIGURE 2: Dependence of light-induced steady-state electrochromic shift parameters in thylakoids on ionic strength (*I*). Data were taken from the curves shown in Figure 1. The steady-state ECS value [$ECS_{ss}$ (■)] was obtained just prior to the light−dark transition. The extent of field inversion [$ECS_{inv}$ (●)] was taken as the negative of the maximum undershoot after the light−dark transition. The total ECS change upon the light−dark transition [$ECS_t$ (▲)] was the sum of $ECS_{ss}$ and $ECS_{inv}$. The white squares represent the ratio of $ECS_{ss}$ to $ECS_t$.

varying concentrations of KCl on the light-induced kinetics of the ECS. When thylakoids suspended in low-salt buffer, with an ionic strength of ~5 mM, were illuminated with 300 $\mu$mol of photons $m^{-2}$ $s^{-1}$, a rapid increase in the ECS was followed by a gradual decrease to a steady-state level, termed the $ECS_{ss}$, which persisted for more than 40 s. This indicates that at least some $\Delta\psi$ can be held for extended periods in a low-salt medium.

After illumination was stopped, ECS rapidly fell to a value below the dark baseline. The difference between the baseline and the lowest extent after the light−dark transition was termed the $ECS_{inv}$. The extent of $ECS_{inv}$ is related to ΔpH. The light−dark transition nearly instantly halted light-driven proton pumping, but proton efflux continued as long as *pmf* > 0. If the initial proton efflux is more rapid than the movement of counterions, net movement of the positively charged protons will cause an electric field "inversion", i.e., a $\Delta\psi$ positive on the stromal side of the membrane (see the discussion in ref *14*). Since, at baseline, $\Delta\psi$ is equal to zero, the magnitude of the field inversion, $ECS_{inv}$, should be proportional to the proton diffusion potential (ΔpH) alone. There is considerable experimental data supporting this general sequence of events (e.g., refs *17* and *18*), but the quantitative implications of these kinetics have not been fully explored. In Figure 1, $ECS_{inv}$ indicates a substantial ΔpH was generated by illumination.

Increasing the KCl concentration decreased the extent of $ECS_{ss}$, completely eliminating it by 50−100 mM salts. In contrast, $ECS_{inv}$ was relatively insensitive to salt. The halftime for recovery of $ECS_{inv}$ to baseline decreased with *I* (or KCl concentration), from about 25 s at 5 mM to 7 s at 105 mM. The total change of the the ECS from the steady state to the full extent of field inversion, i.e., $ECS_{ss} - ECS_{inv}$, termed $ECS_t$, decreased with increasing salt concentrations. The kinetics of decay from $ECS_{ss}$ to $ECS_{inv}$ were constant at 19−22 ms between 5 and 55 mM KCl, but decreased to 12 ms at 105 mM, coincident with a slight decrease in the extent of $ECS_{inv}$.

The light-induced ECS kinetics at low salt concentrations (Figure 1) was strikingly similar to the $\Delta\psi$ kinetics reported by Remiš et al. (*79*), using glass microelectrodes in giant chloroplasts of *P. metallia*. In contrast, the data of Vredenberg and co-workers (*17*, and references therein) and Bulychev et al. (*80*), also obtained with microelectrodes, showed 20−100-fold more rapid kinetic features, while the steady-state magnitude of $\Delta\psi$ was considerably smaller and $\Delta\psi_{inv}$ appeared to be truncated (compare Figure 2.10 of ref *18* and Figure 2 of ref *80* with Figure 2 of ref *79* or Figure 1 in this work). As will become apparent below, all of these features can be explained by high ionic strengths. It may be important that the electrodes used in the study of Remiš et al. (*79*) were filled with 1 M cholate-chloride, while those of Bulychev et al. (*80*) and Vredenburg and co-workers (reviewed in ref *14*) were filled with 2.5 M KCl.

The dependence of kinetics and extents of ECS parameters on the concentration of added $MgCl_2$ was nearly identical to that seen in Figures 1 and 2, except they were 2−3-fold more sensitive to $MgCl_2$ than to KCl concentration (not shown). We conclude that *pmf* parsing is sensitive to ionic strength. These data are also consistent with $P_{Mg^{2+}} \approx P_{K^+}$ (see above).

*Simulations of Transthylakoid $\Delta\psi$ and ΔpH Storage*. The purpose of our simulations was to test the potential role of ionic strength on the parsing of *pmf* into $\Delta\psi$ and ΔpH, and not to mimic all of the nuances of photosynthesis. Consequently, a number of simplifications were made (see above). There are two notable differences between our calculations and those of Vredenburg and co-workers (*17*). First, we used CCCP-containing and $CF_1$-depleted (not shown) systems to avoid the complexities of ATP synthase activation. Second, we assumed that counterion flux was proportional to overall concentration and $\Delta\tilde{\mu}_i$ (eq 2). In fact, the actual kinetic behavior will depend on the specific mechanism for the transporters that are involved, and these have not been sufficiently characterized to fully model. We note that our treatment well accounts for available data on $Cl^-$ channels (*81*), but future refinements will be necessary to fully account for the slight rectifying nature of thylakoid cation channels (*59*). Likewise, the effects of a thylakoid $Ca^{2+}/H^+$ antiporter, as demonstrated by Ettinger et al. (*82*), are beyond the simple model described here. Nevertheless, as will be shown below, our simple model naturally predicts the behavior of isolated thylakoids when literature values for the input parameters were used. Moreover, we will show that even large changes in these kinetic parameters have marginal effects on the parsing of *pmf* into $\Delta\psi$ and ΔpH in the steady state, where the thermodynamic interaction among $\Delta\tilde{\mu}_i$, $\Delta\psi$, and ΔpH, rather than kinetic considerations, will dominate.

*Effects of Varying Ionic Strengths.* The effects of ionic strength on light-induced kinetics of $\Delta\psi$ (Figure 3A), *pmf* (Figure 3B), and ΔpH (Figure 3C) at a range of KCl concentrations were simulated for 135 s light exposure using the above model and parameters. Figure 4 shows the KCl concentration dependence of steady-state transthylakoid $\Delta\psi$ ($\Delta\psi_{ss}$), ΔpH ($\Delta pH_{ss}$), and *pmf* ($pmf_{ss}$) as well as the extents of field inversion ($\Delta\psi_{inv}$) and the total changes in $\Delta\psi$ ($\Delta\psi_t$) upon light−dark transitions. In all cases, ΔpH values were scaled by 2.3*RT*/*F* and expressed in volts.

At 5 mM KCl, ~40% of the *pmf* was stored as $\Delta\psi$ in the steady state. Increasing the KCl concentration from 5 to 105

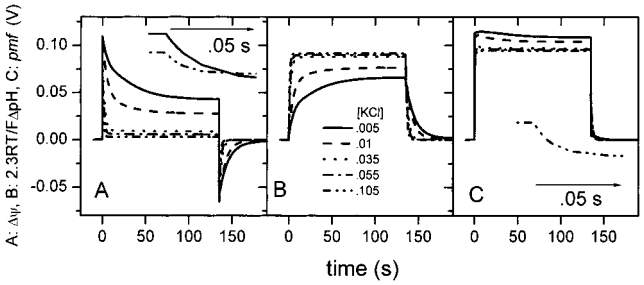


FIGURE 3: Numerical simulations of the effects of ionic strength on transthylakoid *pmf* parameters. Iterative simulations were performed as described in the text, using the following input parameters. Simulated data were stored at 100 $\mu$s intervals during the first 10 ms following dark−light or light−dark transitions, and at 20 ms intervals thereafter: (A) $\Delta\psi$, (B) (2.3*RT*/*F*)$\Delta$pH, and (C) total *pmf*. The simulated ionic strength (i.e., [KCl]) was set at 5 (—), 10 (− − −), 30 (- - -), 55 (— - —), and 105 mM (— - - —). Corresponding line types are also indicated in panel B. The insets of panels A and C indicate the rapid decay kinetics, upon the light−dark transition, of $\Delta\psi$ and *pmf*, respectively, for 5 (—) and 105 mM (— - - —), respectively. The arrows immediately above and below the insets in panels A and C, respectively, indicate the time scale of these curves. The *Y*-axes of the insets were expanded to best illustrate the decay kinetics and are thus in arbitrary units.

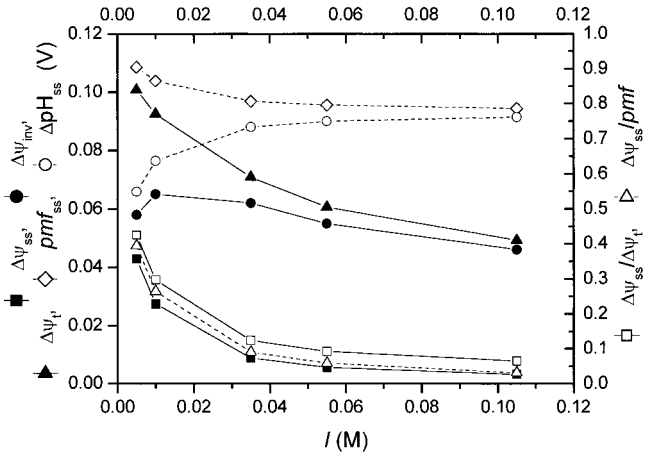


FIGURE 4: Dependence of simulated light-induced transthylakoid *pmf* parameters on ionic strength (*I*). Data were taken from the simulated curves shown in Figure 3. The steady-state $\Delta\psi$ value [$\Delta\psi_{ss}$ (■)] was obtained just prior to the light−dark transition. The extent of field inversion [$\Delta\psi_{inv}$ (●)] was taken as the negative of the maximum undershoot after the light−dark transition. The total $\Delta\psi$ change upon the light−dark transition [$\Delta\psi_t$ (▲)] was the sum of $\Delta\psi_{ss}$ and $\Delta\psi_{inv}$. The white squares represent the ratio of $\Delta\psi_{ss}$ to $\Delta\psi_t$. The steady-state (2.3*RT*/*F*)$\Delta$pH ($\Delta pH_{ss}$) values are shown with the white circles, while the total steady-state *pmf* ($pmf_{ss}$) values are shown with the white diamonds. The values of the fraction of *pmf* stored as $\Delta\psi$ in the steady state, i.e., the ratio of $\Delta\psi_{ss}$ to $pmf_{ss}$, are shown with the white triangles.

mM led to a progressive decrease in $\Delta\psi_{ss}$, from 45 mV to negligible. Meanwhile, $\Delta pH_{ss}$ increased from ~60 to 90 mV. The increase in $\Delta$pH with increasing KCl concentration did not completely compensate for the decrease in $\Delta\psi_{ss}$, resulting in a decrease in $pmf_{ss}$, from about 115 to about 80 mV, as the KCl concentration was increased from 5 to 105 mM. This resulted from the lumen pH-imposed control of photosynthetic electron transfer with a p$K_a$ of 5.5 (see above).

At $I = 5$ mM, simulated $\Delta\psi_{inv}$ was within 90% of (2.3*RT*/*F*)$\Delta pH_{ss}$, indicating that just after the light−dark transition, the poise of $\Delta$pH was nearly canceled by the inverted field. However, $\Delta\psi_{inv}$ dropped to about 50% of (2.3*RT*/*F*)$\Delta pH_{ss}$ at $I = 105$ mM. In effect, more rapid counterion movements masked $\Delta\psi_{inv}$, essentially, by "truncating" the decay curve and by decreasing half-times for decay of $\Delta\psi_{ss}$ to $\Delta\psi_{inv}$, from 17 to 7.5 ms between $I = 5$ and 105 mM (see the inset of Figure 3A for expanded decay kinetics at 5 and 105 mM). The half-times for decay of $\Delta\psi_{inv}$ and $\Delta pH_{ss}$ to baseline also decreased, from ~10 s at $I = 5$ mM KCl to ~2 s at $I = 105$ mM KCl. This was expected because a large $\Delta\psi_{inv}$ will decrease *pmf*, slowing the dissipation of $\Delta$pH, as indicated in the decay kinetics of $pmf_{ss}$. In addition, the half-times for the establishment of steady-state conditions upon the dark−light transition decreased from ~15 to 3 s, as *I* was increased from 5 to 105 mM, reflecting the increased rate of ion fluxes.

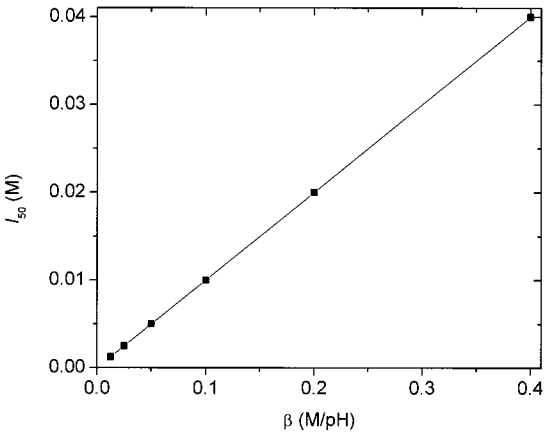


FIGURE 5: Simulated dependence of the ionic strength required to dissipate $\Delta\psi_{ss}$ by 50% on the buffering capacity ($\beta$) of the thylakoid lumen. Simulations were carried out at a range of ionic strengths (from 0 to 0.1 M), as in Figure 3, except that *I* was held constant at 50 mM, while $\beta$ was changed from 12.5 to 40 mM. The ionic strength at which $\Delta\psi_{ss}/pmf$ reached 0.5, $I_{50}$, was estimated from plots as in Figure 4 (△). A linear relationship, passing through the origin, with a slope $I_{50}/\beta$ of 0.1.

*Effects of Varying Model Parameters on the Extents and Kinetics of* $\Delta pH$ *and* $\Delta\psi$. Each of the model parameters was independently varied to determine which were the most important for controlling the kinetics and parsing of *pmf*. The lumen surface/volume ratio had only small effects on both the parsing and kinetics of *pmf* storage (not shown). Likewise, increasing or decreasing the membrane capacitance by 1 order of magnitude had only small effects on *pmf* parameters, because the number of charges stored across the thylakoid always remained much smaller than the number of buffered protons (not shown).

Next to *I*, $\beta$ had the most important effect on the parsing of *pmf*. Figure 5 shows that there is a linear relationship between $\beta$ and the *I* required to dissipate half of the $\Delta\psi$, i.e., that which gave a $\Delta\psi/pmf$ of 0.5, which we call $I_{50}$.

Figure 6 shows the simulated effects of changing ion permeability ($P_{Cl^-}$ and $P_{K^+}$) while maintaining the KCl concentration at 10 mM. Changes in $P_{Cl^-}$ and $P_{K^+}$ of 3 orders of magnitude had no effect on steady-state *pmf*, $\Delta$pH, or $\Delta\psi$. This is because, in a true steady state, the diffusion potential of the ions will reach local equilibrium with $\Delta\psi$ and thus kinetic factors will become insignificant. Increasing $P_{Cl^-}$ and $P_{K^+}$ had large effects on the kinetics of establishment of steady-state conditions, from ~30 s to a few seconds.

*Kinetics of Light-Induced ECS in Intact Leaves*. Figure 7 shows typical ECS kinetic traces from an intact spinach leaf illuminated for either 6 or 65 s with 300 $\mu$mol of photons

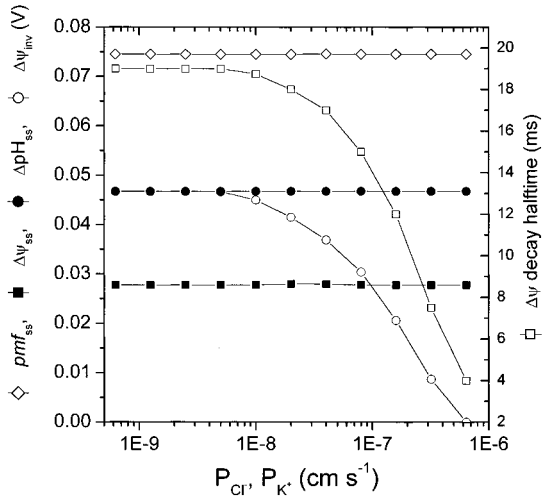


FIGURE 6: Simulated effects of ion permeability on the parsing of transthylakoid *pmf* into $\Delta\psi$ and $\Delta$pH. Numerical simulations were performed as described in the legend of Figure 3, except that [KCl] = 10 mM, $\beta = 0.05$, $pK_{reg} = 6.5$, and the permeabilities of $Cl^-$ and $K^+$ were set equal to each other over a range of values from $0.5 \times 10^{-9}$ to $5 \times 10^{-7}$ cm $s^{-1}$. The values of $pmf_{ss}$, $\Delta\psi_{ss}$, $(2.3RT/F)\Delta pH_{ss}$, and $\Delta\psi_{inv}$ are shown with the white diamonds, black squares, white circles, and black circles, respectively. The half-time values for decay of $\Delta\psi_{ss}$ to $\Delta\psi_{inv}$ are shown with the white squares.

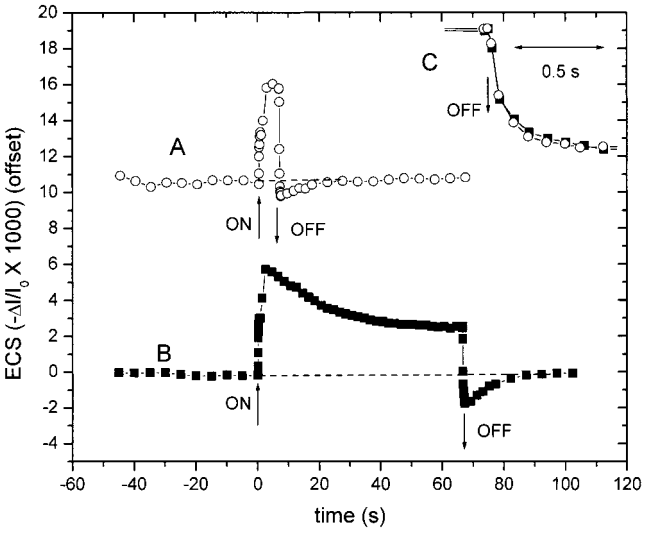


FIGURE 7: Light-induced electrochromic shift (ECS) signals in an intact spinach leaf. An intact spinach leaf was placed in the diffused optics flash spectrophotometer (DOFS) and illuminated with 300 $\mu$mol of photons $m^{-2}$ $s^{-1}$ for either 6 s [trace A (○)] or 65 s [trace B (■)], and the ECS signal was measured and deconvoluted as described in the text. The data were offset to allow clear visualization of both traces. The inset (C traces) shows an expanded view of the ECS decay kinetics upon the light−dark transition. To allow good comparisons of decay kinetics, traces A and B were normalized by eye to their full extents of $ECS_t$.

$m^{-2}$ $s^{-1}$. The data were averages of four separate traces and taken in alternating order, with a 2 min dark adaptation between each light exposure to ensure that the physiological status of the leaf was constant. The 65 s illumination trace appeared very similar to those reported previously by us in *Solanum nigram* leaves (*27*) except that the induction upon illumination was more complex in our earlier work. This likely resulted from the relatively short dark adaptation times used in this work, which presumably maintained Calvin−Benson cycle enzymes in their active forms. In addition, the kinetic and steady-state features of ECS in the leaf were strikingly similar to those observed in isolated thylakoids at low *I* (or KCl concentration) (compare with Figure 1). After a brief (6 s) illumination, *pmf* was stored almost exclusively as $\Delta\psi$, as indicated by the small extent of $ECS_{inv}$. With longer illumination, $ECS_{ss}$ gradually decreased after an initial spike, with a half-time of ∼10−15 s, to a value of about 2.5 units. Upon the light−dark transition, ECS fell sharply with a half-time of ∼20 ms to an $ECS_{inv}$ value of ∼1.75 units. $ECS_{inv}$ then decayed to baseline with a half-time of ∼10 s. When offset and normalized, the ECS decay kinetics after illumination for 6 and 65 s were nearly superimposable.

## DISCUSSION

Our previous arguments (*22*) about the steady-state pH of the chloroplast lumen fell into two distinct categories. Those based on the turnover rates and stabilities of lumen enzymes suggested that the lumen pH remained above ∼5.8. On the other hand, arguments based on the energy in *pmf* needed to activate the ATP synthase and maintain $\Delta G_{ATP}$ suggested that the pH remained well below 5.5. One of the main assumptions in the energetics argument was that all *pmf* was stored as $\Delta$pH. However, even a small contribution of $\Delta\psi$ to $pmf_{ss}$ (∼30 mV, equivalent to ∼0.5 pH unit) could reconcile the two arguments.

With respect to this line of reasoning, we asked the following five major questions in this work. (1) Under what conditions can $\Delta\psi$ be stably stored across the thylakoid membrane? (2) Are the conditions favorable for $\Delta\psi$ storage likely to be physiological? (3) Can the ECS be used to monitor $\Delta\psi$ and $\Delta$pH in vitro and in vivo? (4) Are ECS measurements in intact plants compatible with a substantial fraction of $\Delta\psi$ storage? (5) What are the possible implications of $\Delta\psi$ storage for the control of regulation of photosynthesis?

Experiments performed on isolated spinach thylakoids (Figures 1 and 2) demonstrated that a significant fraction of transthylakoid *pmf* can be stored as $\Delta\psi$ for extended periods of time, most likely indefinitely, provided that activities of ions permeable to the thylakoid membrane was kept low, consistent with earlier results (*10*−*13*). However, these experiments alone were inadequate for defining other parameters that might influence storage. We turned to computer simulations not only to give us an idea of what factors control $\Delta\psi$ storage but also to confirm our observations about the effect of *I*. Extensive simulations, using a simplified flux model and literature values for thylakoid properties, suggested that the parsing of *pmf* into $\Delta\psi$ and $\Delta$pH is controlled mainly by two main parameters: (1) the ionic strength of permeable ions (Figures 3 and 4), and (2) the lumen buffering capacity (Figure 5).

The dependence of $\Delta\psi_{ss}$ on *I*, observed both in simulations (Figures 3 and 4) and in vitro (i.e., measured as $ECS_{ss}$, Figures 1 and 2), is consistent with the prevailing, and well-established, hypothesis that $\Delta\psi$ is dissipated by counterion fluxes. In the steady state, $\Delta\psi$ will come into equilibrium with the diffusion potentials of the counterion pools. To mask the $\Delta\psi$ created by $H^+$ influx, stoichiometric net movements of charges must occur across the thylakoid membrane. The resulting differential ion concentrations will create a diffusion

potential that will hinder further ion movements. It follows that $\Delta\psi_{ss}$ will depend on the initial ionic strength and on the net proton flux into the lumen. The latter is dependent on $\beta$ because this will determine the "proton load" needed to acidify the lumen by a particular extent (Figure 5). Altering other thylakoid properties, including membrane capacitance and individual ion permeabilities, had only small effects on the magnitudes of simulation *pmf* components in the steady state.

*Comparisons of in Vitro ECS Assays with Simulations.* One of the most remarkable features of the above simulations is that, using parameters obtained from the literature, they very closely match the results of the thylakoid experiments described in Figures 1 and 2 without further manipulation. In Figure 1, at $I \approx 5$ mM, an initial spike in ECS was followed by a gradual decline to about half the maximum value with a half-time of ~10 s. This was very similar to the 5 mM KCl simulations depicted in Figure 3, except that the decline to the steady-state levels was ~3-fold slower (note the different time scale for the simulations). In simulations, the decline was due to acidification of the lumen, which restricted electron flow at the cyt $b_6f$ complex. This likely holds for the thylakoid system as well (see the review in ref *24*). When the sample was held in the dark, $ECS_{ss}$ declined rapidly with a half-time of ~20 ms to an $ECS_{inv}$ value that was about equal to $ECS_{ss}$. This was very similar to the kinetics of $\Delta\psi$ in the simulations at $I = 5$ mM. The recovery from $ECS_{inv}$ to baseline had a half-time of ~15 s, whereas the simulations were again ~3-fold slower. The increase in decay rates could possibly reflect the underestimation of $P_{K^+}$ and $P_{Cl^-}$ in our model. Yet, as suggested by simulations where ion permeability was altered (Figure 6), this should not affect the relative, steady-state extents of $\Delta\psi$ and $\Delta$pH. In agreement with this prediction, the extents of $ECS_{ss}$, $ECS_{inv}$, and $ECS_t$ (in thylakoids) and $\Delta\psi_{ss}$, $\Delta\psi_{inv}$, and $\Delta\psi_t$ (in simulations) had almost identical (relative) dependencies on KCl concentration (*I*), as did the $ECS_{ss}/ECS_t$ and $\Delta\psi_{ss}/\Delta\psi_t$ ratios (Figures 2 and 4).

*Estimations of $\Delta$pH Based on $ECS_{inv}$.* The simulations described in Figures 4 and 6 show that, when ion fluxes are substantially slower than that of protons during the initial decay in a light−dark transition, the magnitude of $\Delta\psi_{inv}$ is expected to closely reflect the $\Delta$pH component of *pmf*. On the other hand, at high ionic permeabilities (Figure 6), as in the presence of valinomycin, or at high *I* (Figure 4), $\Delta\psi_{inv}$ will be masked by counterion movements and $\Delta\psi_{inv}$ will significantly underestimate $\Delta$pH. It is thus clear that the extent of $\Delta\psi_{inv}$ will provide a reasonable estimate of $\Delta$pH when counterion fluxes are significantly slower than proton fluxes, but not when rapid ion movements effectively compete with proton flux. It should, though, be possible to assess the extents of such competition by its effect on $\Delta\psi_{ss} \rightarrow \Delta\psi_{inv}$ or $\Delta\psi_{inv} \rightarrow$ baseline decay kinetics. The close correlation of in vitro ECS kinetics with the simulated $\Delta\psi$ (Figures 2 and 4) led us to conclude that at low *I* (5 mM), $ECS_{inv}$ should be within ~10% of $\Delta$pH, while at 105 mM KCl, it may give an estimate ~50% lower than the true $\Delta$pH.

Another potentially useful parameter is $\Delta\psi_{ss}/\Delta\psi_t$, which should reflect the fraction of *pmf* stored as $\Delta\psi$ (i.e., $\Delta\psi_{ss}/pmf$). $\Delta\psi_{ss}/\Delta\psi_t$ had a dependence on *I* almost identical to that of $\Delta\psi_{ss}/pmf_t$, because the errors in estimating $\Delta pH_{ss}$ from $\Delta\psi_{inv}$ were largest when $\Delta\psi$ was nearly completely masked. We thus argue that $ECS_{ss}/ECS_t$ represents a reasonable estimate of the fraction of *pmf* stored as $\Delta\psi$, over a broad range of *I*, in the absence of exogenously added ionophores (see Figure 6). Using this estimate, and the data in Figure 2, we suggest that thylakoids suspended in a medium with an *I* of 5 mM store ~40% of *pmf* as $\Delta\psi$, and that this fraction decreases with a half-effective *I* of ~20 mM. As typical thylakoid resuspension buffers have *I* values of >50 mM, we conclude that most in vitro assays have been conducted under conditions where *pmf* is stored almost exclusively as $\Delta$pH.

*Parsing of pmf in Vitro.* Order of magnitude comparisons of our simulations and in vitro assays with literature estimates of $pmf_{ss}$ would be a useful first-order assessment of the relevance of our work. In our thylakoid preparations, a fully saturating flash produced an ECS of about $1.4 \times 10^{-3}$ $\Delta I/I_0$ unit (not shown). Literature estimates of $\Delta\psi$ produced by a single-turnover flash range from ~25 to 100 mV (see the review in ref *29*). Considering that $ECS_t$ reached $2.5 \times 10^{-3}$ unit at low *I*, where dissipation of $\Delta\psi_{inv}$ should have been small, we estimate a steady-state *pmf* in our thylakoids of 45−180 mV, spanning the *pmf* range predicted from $\Delta$pH (*48*) and $\Delta G_{ATP}$ measurements (see ref *22*). At $I = 5$ mM, $\Delta\psi_{ss}$ could be estimated to be between 16 and 63 mV. Under the same conditions, the simulations produced somewhat lower *pmf* values, from 80 to 110 mV. Given the significant degrees of freedom in our calculations, and in the estimates of the slope of ECS versus $\Delta\psi$, we conclude that both our in vitro assays and simulations yielded reasonable extents of *pmf*.

*pmf in Vivo.* Consistent with our earlier results (*27*), Figure 7 shows that even after illumination for 65 s a significant, positive $ECS_{ss}$ remained in intact spinach leaves. This observation suggests that, as in thylakoids, a substantial fraction of *pmf* can be stored as $\Delta\psi$ in vivo, at least under the conditions used in our assays. The chlorophyll contents of intact leaves (~25−35 $\mu$g/cm$^2$) were, on the basis of probed area, roughly 2-fold higher than those of our thylakoid suspensions (~20 $\mu$g/mL with a a path length of 1 cm). When scaled by this factor, the amplitude of light-induced $ECS_{ss}$ was within a factor of 2 of that observed in the thylakoids at an *I* of 5 mM (Figure 1). We take this as strong evidence that $\Delta\psi_{ss}$ is roughly 25−100 mV higher after exposure for 65 s to 300 $\mu$mol of photons m$^{-2}$ s$^{-1}$ than in the dark. Microelectrode experiments (e.g., ref *79*) show considerably lower amplitudes of $\Delta\psi$, but since both electrode sealing and placement will affect the amplitudes of the signals, it is difficult to ascertain whether the reported values are quantitative representations of true $\Delta\psi$. The significant $\Delta\psi_{ss}$ estimated from our experiments is likely due to a low in vivo chloroplast *I*, as both the establishment of $\Delta\psi_{ss}$ and the recovery of $ECS_{inv}$ were quite slow (>15 s), as observed in vitro at $I < 10$ mM (Figures 1 and 2).

The next obvious question is what fraction of *pmf* is stored as $\Delta\psi$, in vivo? Judging from the slow recovery of $ECS_{inv}$ to baseline and the stable $\Delta\psi_{ss}$ (Figure 7), we expect that the concentrations and permeabilities of ions in the chloroplast in vivo are low. At first glance, this appears to indicate that $ECS_{inv}$ can safely be used as a probe of $\Delta$pH in vivo. However, we must also consider the effects of ATP synthase regulation. The ATP synthase is kinetically disabled when the membrane is not energized, presumably to prevent ATP

hydrolysis in the dark (*61*, *83*, *84*). It is activated when the *pmf* was increased over the activation threshold level, which, in turn, is modulated by thioredoxin-mediated redox chemistry. In the dark, a pair of cysteines in the $\gamma$-subunit of the ATP synthase are oxidized coordinately, forming a disulfide bridge, while in the light, the disulfide bridge is reduced by thioredoxin. In isolated thylakoids, the *pmf* required to activate the complexes in the oxidized form was found to be energetically equivalent to $\sim$2−3 pH units, while that required to activate the reduced form was about 1 pH unit lower (*2*, *61*). In dark-adapted intact leaves, this regulatory behavior is reflected as a distinct slowing of the ECS decay kinetics as the extent of the signal decays (*29*, *85*). In contrast, the conditions used in this work strongly favored the ATP synthase in its reduced form (*85*). Under these in vivo conditions, the ATP synthase is highly conductive to protons, and most, but not all, of the ECS decays after single-turnover flash excitation (*29*). Our simulations indicate that the slowly recovering phase would almost certainly be masked by counterion fluxes, leading to an underestimate of $\Delta$pH from $ECS_{inv}$.

To test for kinetic effects of ATP synthase regulation, we compared ECS decay kinetics after short (6 s) and long (65 s) illuminations, where both the amplitudes of *pmf* and its apparent parsing into $\Delta$pH and $\Delta\psi$ differed. Figure 7 shows that ECS decay kinetics observed after illumination for 3 or 65 s were nearly identical. This strongly suggests that the conductivities of protons (through the ATP synthase) and counterions (through channels) were similar under both conditions. By extrapolation, this implies that, despite the apparent change in *pmf* parsing (from nearly essentially all $\Delta\psi$ after 6 s to $\sim$50% $\Delta$pH at 65 s), and the $\sim$1.5-fold difference in $ECS_t$ amplitudes for the two illumination conditions, the force−flux relationship at the ATP synthase was essentially unchanged. We have observed similar behavior during steady-state illumination of intact spinach leaves, where the half-time for decay of ECS was unchanged by light intensity over a wide range, where the amplitude of $ECS_t$ differed by a factor of $\sim$10 (*56*). This suggests that, in contrast to dark-adapted plants illuminated with flashes, under conditions more resembling the steady state, the ATP synthase remained active during essentially the entire ECS decay. This could be explained if, under our conditions, ATP hydrolysis in the dark maintained the *pmf* above the activation threshold for the ATP synthase between illumination periods. In this case, our baseline ECS value would represent the basal (or dark) *pmf*. Indeed, the existence of a dark or basal *pmf* has been inferred from studies of green algae (*25*, *26*), as well as higher plants (*29*). If such a basal *pmf* is generated by reversal of the ATP synthase reaction, then its magnitude would approach $\Delta G_{ATP}/n$ in the dark. If it is assumed that $\Delta G_{ATP}$ does not change appreciably during illumination, as expected from literature estimates (e.g., ref *86*), light-driven ECS changes would still be comparable to each other. Thus, $ECS_{ss}$ and $ECS_{inv}$ would not reflect the absolute values of $\Delta\psi$ and $\Delta$pH, but instead would represent the light−dark differences in these values. Using the estimates of the relationship between $\Delta\psi$ and ECS given above, we estimate that illumination of chloroplasts in intact spinach plants increases transthylakoid *pmf* between 60 and 190 mV. Of course, this does not include contributions from basal *pmf*.

Another approach to estimating in vivo, steady-state $\Delta\psi$ would be to use ECS kinetics to estimate the fraction of *pmf* stored as $\Delta\psi$, and back-calculate from estimates of $\Delta G_{ATP}$. If no truncation of $ECS_{inv}$ occurred, the data in Figure 7 suggest that $\sim$50% of *pmf* was stored as $\Delta\psi$. Given our in vitro experiments, it is likely that from 10 to 50% of $ECS_{inv}$ was truncated. Using a conservative estimate of 30% of *pmf* stored as $\Delta\psi$, and assuming near-equilibrium between *pmf* and $\Delta G_{ATP}$, and a $\Delta G_{ATP}$ of 45 kJ/mol, a stroma pH of 7.5, and an $H^+$/ATP (*n*) ratio of 4 (see the review in ref *22*), the lumen pH should reach $\sim$6.1. This is in agreement with the range predicted from estimates of lumenal enzyme kinetics and stabilities (*22*).

*Ionic Strength of the Chloroplast.* We have presented data suggesting that, in vivo, a significant $\Delta\psi_{ss}$ is held across the thylakoid membrane. The simplest way to explain these results is that the ionic strength of thylakoid membrane-permeable ions (most likely $Mg^{2+}$, $Cl^-$, and $K^+$) in the chloroplast is fairly low (<10 mM). The literature on the chloroplast ionic balance and permeability remains confusing. Measured $Mg^{2+}$ concentrations ranged from 2 to 18 mM, a significant fraction of which is expected to be bound to the membrane, LHC complexes, and nucleotides (*87*, *88*). Recent measurements show very low $Cl^-$ content and activity, from $\sim$1−3 mM (*87*, *89*). $K^+$ concentrations varied from about $\sim$20−30 mM (see reviews in refs *88* and *90*) to 180 mM (*87*). However, much of the $K^+$ appears to be bound or sequestered in the chloroplast (*88*, *91*, *92*) and does not diffuse out of the envelope even in the presence of high concentrations of valinomycin. Similarly, the chloroplast preparations of Schröppel-Meier and Kaier (*87*) retained essentially all $K^+$ for up to 10 min when suspended in a low-salt medium, despite the fact that cation and anion channels are both present and probably active (but see below) in the thylakoid envelopes (*93*−*98*). Possible explanations for this behavior include a strong Donnan potential in the stroma (due to its high protein content) (*88*) or chelation by impermeable species, effectively lowering the activity of free $K^+$. The experiments of Schröppel-Meier and Kaiser (*87*) were conducted using atomic absorption spectroscopy on boiled preparations, and did not distinguish between free and bound ions. We emphasize that it is the activity of free ions, rather than the total ion content, that will determine the dissipation of $\Delta\psi$.

Further complications come from the fact that the chloroplast inner envelope is energized by ATP-driven proton pumps, with clear indications of active ion transport processes (*64*, *95*, *99*−*102*). The pumping of protons from the stroma to the cytoplasm is light-activated, and probably dependent upon photosynthesis (reviewed in refs *90* and *103*). The outward pumping of protons sets up a transenvelope *pmf*, which drives $K^+$ and $Mg^{2+}$ influx (to the stroma) (*90*) and $Cl^-$ efflux (from the stroma) (*103*, *104*). These may be critical, since counterion movements would tend to *maintain* transthylakoid $\Delta\psi$ by counteracting the thylakoid *pmf*-induced counterion fluxes. Indeed, the ion movements caused by inner envelope energization, by themselves, would be expected to establish a transthylakoid $\Delta\psi$ positive on the lumen side. Regardless, the presence of these light-dependent processes would imply that chloroplast ionic balance is held out of equilibrium with its surroundings, making it difficult to extrapolate physiologically relevant

ion concentrations from isolated material (see the discussion in ref *91*).

Another important consideration is the possibility of lumen volume changes, which our simple thylakoid model did not allow. Light-induced effluxes of cations would tend to shrink the thylakoid, but since lumen volume is already very small, further changes would be very limited. In contrast, counterfluxes of $Cl^-$ can swell thylakoids up to 50-fold (*88*, *103*), essentially diluting the ensuing $Cl^-$ diffusion potential, and allowing further dissipation of $\Delta\psi$. Moreover, the differential effects of anion and cation fluxes on lumen volume imply that a low $Cl^-$ concentration would be more critical for maintaining $\Delta\psi$ than low cation concentrations. In line with this argument, there is evidence that thylakoids in situ shrink upon illumination (*105*), consistent with light-induced cation efflux. Furthermore, the differential effects of specific ionophores point toward $Mg^{2+}$ being the predominant mobile counterion in chloroplasts (*92*) (this also contradicts a high concentration of free $K^+$; see above and the discussion in ref *88*).

Considerable early work was carried out to determine the effects of ionic strength and balance on electron transfer (*88*). The concentration of $Mg^{2+}$ appeared to have the greatest effect, because it is required for granal stacking, which affects the efficiency of light harvesting (*88*). In addition, extensive depletion of $Ca^{2+}$ or $Cl^-$ (in the micromolar range) inhibits PS II at the level of the oxygen-evolving complex (*106*). On the other extreme, high salt concentrations ($I > 0.1$ M) have been shown to inhibit photosynthesis at the level of the photosystems (*107*) and intermediate electron transfer (*108*). The ionic concentrations used in this study are such that none of these extreme effects are expected.

We conclude that little is unambiguously known about the true ionic content of chloroplasts in vivo. Our data on dark-adapted leaves, illuminated for ~1 min, are consistent with activities of permeable ions low enough to allow significant $\Delta\psi_{ss}$, i.e., probably less than ~10 mM, but sufficiently high to allow granal stacking and efficient electron transfer. Obviously, more work is needed to settle these issues.

*Effects of pmf Parsing on Regulation or Control of Photosynthesis.* Finally, differential parsing of *pmf* into $\Delta\psi$ and $\Delta$pH is expected to have large effects on the control or regulation of photosynthesis. Storage of *pmf* as $\Delta$pH, with the resulting acidification of the lumen, is known to affect the turnover rates of key photosynthetic enzymes and initiate downregulatory processes (*22*), whereas $\Delta\psi$ appears to have a less significant effect on these processes (*26*). Thus, in our simulations (Figures 3 and 4), dissipation of $\Delta\psi$ by counterion fluxes results in slower electron transfer, and thus lower $pmf_{ss}$.

The higher the value of the regulatory p$K_a$, the larger will be the effect of differential *pmf* parsing into $\Delta\psi$ and $\Delta$pH. In our simulations, a regulatory p$K_a$ of 5.5 was chosen because this best reflected the behavior of the rate limitation at the cyt $b_6f$ complex. Yet, the half-time for turnover of the cyt $b_6f$ complex does not change during illumination under nonstressed conditions (*22*), indicating that light collection by the antenna complexes is regulated to keep the lumen pH above ~5.8. In other words, a significantly higher regulatory p$K_a$ normally operates in vivo. Therefore, we suggest that *pmf* parsing will have a large effect on the activity of lumen pH-driven regulatory phenomena.

We further suggest that differential parsing of *pmf* modulates downregulatory processes by *pmf*. Such changes could take effect when stress conditions induce, through active or passive processes, a change in the ionic strength of the chloroplast, thereby shifting pH regulation. A second possibility is that the chloroplast may actively change the buffering capacity of the lumen. However, this seems less likely as the buffering groups are thought to reside on amino acid residues and a large change in lumen protein concentrations would be required.

## CONCLUSIONS

We have presented evidence that a substantial fraction of transthylakoid *pmf* is stored, at least under some in vivo conditions, as $\Delta\psi$. This $\Delta\psi$, estimated to be between 25 and 100 mV after a 65 s illumination at 300 $\mu$mol of photons $m^{-2}$ $s^{-1}$, would allow a *pmf* sufficient for maintaining observed levels of $\Delta G_{ATP}$ with a moderate lumen pH (>5.8) (*22*). We further argue that differential parsing of *pmf* into $\Delta$pH and $\Delta\psi$ will have large effects on the regulatory behavior of the chloroplast. As evidenced by simulations and assays on isolated thylakoids, the simplest mechanism allowing for $\Delta\psi_{ss}$ would be to maintain the low concentrations of thylakoid-permeable ions. We have presented arguments based on the kinetics of light-induced ECS changes that this is the case in vivo.

## ACKNOWLEDGMENT

We thank Drs. G. E. Edwards, B. Ivanov, and S. K. Herbert for important discussions. The excellent technical assistance from M. Jacoby is gratefully acknowledged.

## REFERENCES

1. Mitchell, P. (1966) *Biol. Rev. 41*, 445−502.
2. Hangarter, R. P., and Good, N. D. (1982) *Biochim. Biophys. Acta 681*, 396−404.
3. Kaim, G. D. P. (1998) *EMBO J. 17*, 5887−5895.
4. Kaim, G. D. P. (1998) *FEBS Lett. 434*, 57−60.
5. Dimroth, P. K. G., and Matthey, U. (1998) *Biochim. Biophys. Acta 1365*, 87−92.
6. Fischer, S., and Gräber, P. (1999) *FEBS Lett. 457*, 327−332.
7. Dimroth, P. (2000) *Biochim. Biophys. Acta 1458*, 374−386.
8. Kashket, E. R. (1981) *J. Bacteriol. 146*, 369−376.
9. Booth, I. R. (1985) *Microbiol. Rev. 49*, 359−378.
10. Huber, U. (1980) *Ber. Bunsen-Ges. 84*, 1050−1055.
11. Siggel, U. (1981) *Bioelectrochem. Bioenerg. 8*, 347−354.
12. Tiemann, R., and Witt, H. T. (1982) *Biochim. Biophys. Acta 681*, 201−211.
13. Siggel, U. (1981) in *Photosynthesis I* (Akoyonoglou, G., Ed.) pp 431−442, Balaban International Science Services, Philadelphia.
14. Vredenberg, W. J., and Bulychev, A. A. (1976) *Plant Sci. Lett. 7*, 101−107.
15. Vredenberg, W. J., and Tonk, W. J. M. (1975) *Biochim. Biophys. Acta 387*, 580−587.
16. Bulychev, A. (1984) *Biochim. Biophys. Acta 766*, 747−752.
17. van Kooten, O., Snel, J. F. H., and Vredenberg, W. J. (1986) *Photosynth. Res. 9*, 211−227.
18. Vredenberg, W. J. (1976) in *The Intact Chloroplast* (Barber, J., Ed.) pp 53−87, Elsevier/North-Holland Biomedical Press, Amsterdam.
19. Junge, W., Ausländer, W., McGeer, A. J., and Runge, T. (1979) *Biochim. Biophys. Acta 546*, 121−141.
20. Vredenberg, W. J., and Duysens, L. N. M. (1965) *Biochim. Biophys. Acta 94*, 355−370.
21. Vredenberg, W. J. (1969) *Biochem. Biophys. Res. Commun. 37*, 785−792.

22. Kramer, D. M., Sacksteder, C. A., and Cruz, J. A. (1999) *Photosynth. Res. 60*, 151−163.
23. Tikhonov, A. N., Khomutov, G. B., Ruuge, E. K., and Blumenfeld, L. A. (1981) *Biochim. Biophys. Acta 637*, 321−333.
24. Tikhonov, A. N., and Timoshin, A. A. (1985) *Biol. Membr. 2*, 608−626.
25. Joliot, P., and Joliot, A. (1989) *Biochim. Biophys. Acta 975*, 355−360.
26. Finazzi, G., and Rappaport, F. (1998) *Biochemistry 37*, 9999−10005.
27. Kramer, D. M., and Sacksteder, C. A. (1998) *Photosynth. Res. 56*, 103−112.
28. Junge, W. (1977) in *Encyclopedia of Plant Physiology* (Trebst, A., and Avron, M., Eds.) pp 59−93, Springer-Verlag, New York.
29. Kramer, D. M., and Crofts, A. R. (1989) *Biochim. Biophys. Acta 976*, 28−41.
30. Anderson, B., and Barber, J. (1996) in *Photosynthesis and the Environment* (Baker, N. R., Ed.) pp 101−121, Kluwer Academic Publishers, Dordrecht, The Netherlands.
31. Styring, S., Virgin, I., Ehrenberg, A., and Andersson, B. (1990) *Biochim. Biophys. Acta 1015*, 269.
32. Krieger, A., and Weis, E. (1993) *Photosynth. Res. 37*, 117−130.
33. Spetea, C., Hidge, E., and Vass, I. (1997) *Biochim. Biophys. Acta 1318*, 275−283.
34. Tjus, S. E., Moller, B. L., and Scheller, H. V. (1998) *Plant Physiol. 116*, 755−765.
35. Sonoike, K. (1996) *Plant Sci. 115*, 157−164.
36. Sonoike, K. (1996) *Plant Cell Physiol. 37*, 239−247.
37. Sonoike, K. (1999) *J. Photochem. Photobiol., B 48*, 136−142.
38. Ivanov, B., Kobayashi, Y., Bukhov, N. G., and Heber, U. (1998) *Photosynth. Res. 57*, 61−70.
39. Havaux, M., and Davaud, A. (1994) *Photosynth. Res. 40*, 75−92.
40. Demmig-Adams, B., and Adams, W. W., III (1992) *Annu. Rev. Plant Physiol. Plant Mol. Biol. 43*, 599−626.
41. Demmig-Adams, B., and Adams, W. W., III (1996) *Trends Plant Sci. 1*, 21−26.
42. Horton, P., Ruban, A., and Walters, R. (1996) *Annu. Rev. Plant Physiol. Plant Mol. Biol. 47*, 655−684.
43. Owens, T. G. (1996) in *Photosynthesis and the Environment* (Baker, N., Ed.) pp 1−23, Kluwer Academic Publishers, Dordrecht, The Netherlands.
44. Yamamoto, H. Y., and Bassi, R. (1996) in *Oxygenic Photosynthesis: The Light Reactions* (Ort, D. R., and Yocum, C. F., Eds.) pp 539−563, Kluwer Academic Publishers, Dordrecht, The Netherlands.
45. Delosme, R., Olive, J., and Wollman, F.-A. (1996) *Biochim. Biophys. Acta 1273*, 150−158.
46. Witt, H. T., and Zickler, A. (1974) *FEBS Lett. 39*, 205−208.
47. Witt, H. (1975) *Biochim. Biophys. Acta 505*, 355−427.
48. Tikhonov, A. N., Khomutov, G. B., and Ruuge, E. K. (1984) *Photochem. Photobiol. 8*, 261−269.
49. Nishio, J. N., and Whitmarsh, J. (1990) *Plant Physiol. 95*, 522−528.
50. Rumberg, B., and Siggel, U. (1969) *Naturwissenschaften 56*, 130−132.
51. Witt, H. T. (1979) *Biochim. Biophys. Acta 505*, 355−427.
52. Bendall, D. S. (1982) *Biochim. Biophys. Acta 683*, 119−151.
53. Rich, P. (1982) in *Function of Quinones in Energy Conserving Systems* (Trumpower, B. L., Ed.) pp 73−86, Academic Press, New York.
54. Genty, B., and Harbinson, J. (1996) in *Photosynthesis and the Environment* (Baker, N. R., Ed.) pp 67−99, Kluwer Academic Publishers, Dordrecht, The Netherlands.
55. Nishio, J. N., and Whitmarsh, J. (1993) *Plant Physiol. 101*, 89−96.
56. Sacksteder, C. A., Kanazawa, A., Jacoby, M. E., and Kramer, D. M. (2000) *Proc. Natl. Acad. Sci. U.S.A.* (submitted for publication).
57. Vredenberg, W. J., van Kooten, O., and Snel, J. F. H. (1986) unpublished observations, pp 1−3.
58. Vredenberg, W. J., and Bulychev, A. A. (1976) *Plant Sci. Lett. 7*, 101−107.
59. Pottosin, I. I., and Schönknecht, G. (1996) *J. Membr. Biol. 152*, 223−233.
60. Gräber, P., Fromme, P., Junesch, U., Schmidt, G., and Thulke, G. (1986) *Ber. Bunsen-Ges. 90*, 1034−1040.
61. Junesch, U., and Gräber, P. (1985) *Biochim. Biophys. Acta 809*, 429−434.
62. Junge, W. (1989) *Ann. N.Y. Acad. Sci. 574*, 268−286.
63. Heldt, H. W., Werdan, K., Milovancev, M., and Geller, G. (1973) *Biochim. Biophys. Acta 314*, 224−241.
64. Wu, W., and Berkowitz, G. A. (1992) *Plant Physiol. 98*, 666−672.
65. Junge, W., and McLaughlin, S. (1987) *Biochim. Biophys. Acta 890*, 1−5.
66. van Kooten, O., van Gloudemans, A. G. M., and Vredenberg, W. J. (1983) *Photobiochem. Photobiophys. 6*, 9−14.
67. Staehelin, L. A. (1986) in *Photosynthesis III Photosynthetic Membranes and Light Harvesting Systems* (Staehelin, L. A., and Arntzen, C. J., Eds.) pp 1−84, Springer-Verlag, Berlin.
68. Sacksteder, C. A., and Kramer, D. M. (2000) *Photosynth. Res.* (in press).
69. Kramer, D. M., and Sacksteder, C. A. (1990) *Biochim. Biophys. Acta 1183*, 72−84.
70. Engelbrecht, S., Lill, H., and Junge, W. (1986) *Eur. J. Biochem. 160*, 635−643.
71. Welford, W. T., and Winston, R. (1989) *High Collection Nonimaging Optics*, Academic Press, San Diego.
72. Deamer, D. W., Crofts, A. R., and Packer, L. (1966) *Biochim. Biophys. Acta 131*, 81−96.
73. Heber, U. (1969) *Biochim. Biophys. Acta 180*, 302−319.
74. Sivak, M. N., Dietz, K. J., Heber, U., and Walker, D. A. (1985) *Arch. Biochem. Biophys. 237*, 513−519.
75. Gerst, U., Schonknecht, G., and Heber, U. (1994) *Planta 193*, 421−429.
76. Veljovic-Jovanovic, S., Bilger, W., and Heber, U. (1993) *Planta 191*, 365−376.
77. Bilger, W., Bjorkman, O., and Thayer, S. S. (1989) *Plant Physiol. 91*, 542−551.
78. Shibata, K. (1959) in *Methods of Biochemical Analysis* (Glick, D., Ed.) pp 77−109, Interscience Publishers, New York.
79. Remiš, D., Bluychev, A. A., and Kurella, G. A. (1986) *Biochim. Biophys. Acta 852*, 68−73.
80. Bulychev, A., Andrianov, V. K., Kurella, G. A., and Litvin, F. F. (1971) *Nature 236*, 175−177.
81. Schönknecht, G., Hedrich, R., Junge, W., and Raschke, K. (1988) *Nature 336*, 589−592.
82. Ettinger, W. F., Clear, A. M., Fanning, K. J., and Peck, M. L. (1999) *Plant Physiol. 119*, 1379−1385.
83. Hangarter, R. P., Grandoni, P., and Ort, D. R. (1987) *J. Biol. Chem. 262*, 13513−13519.
84. Ort, D. R., Grandoni, P., Ortiz-Lopez, A., and Hangarter, R. P. (1990) in *Perspectives in Biochemical and Genetic Regulation of Photosynthesis*, pp 159−173, Wiley-Liss, New York.
85. Kramer, D. M., Wise, R. R., Frederick, J. R., Alm, D. M., Hesketh, J. D., Ort, D. R., and Crofts, A. R. (1990) *Photosynth. Res. 26*, 213−222.
86. Giersch, C., Heber, U., Kobayashi, Y., Inoue, Y., Shibata, K., and Heldt, H. W. (1980) *Biochim. Biophys. Acta 590*, 59−73.
87. Schroppel-Meier, G., and Kaiser, W. M. (1988) *Plant Physiol. 87*, 822−827.
88. Barber, J. (1976) in *The Intact Chloroplast* (Barber, J., Ed.) pp 89−134, Elsevier/North-Holland Biomedical Press, Amsterdam.
89. Thaler, M., Simonis, W., and Schönknecht, G. (1992) *Plant Physiol. 99*, 103−110.
90. Gimmler, H., Schäfer, G., and Heber, U. (1974) in *Proceedings of the Third International Congress on Photosynthesis* (Avron, M., Ed.) pp 1381−1392, Elsevier Scientific, Amsterdam.
91. Nakatani, H. Y., Barber, J., and Minski, M. J. (1979) *Biochim. Biophys. Acta 545*, 24−35.

92. Barber, J., Mills, J., and Nicholson, J. (1972) *FEBS Lett. 49*, 106−110.
93. Kaiser, W. M., Urbach, W., and Gimmler, H. (1980) *Plants 143*, 170−175.
94. Pottosin, I. I. (1992) *FEBS Lett. 308*, 87−90.
95. Berkowitz, G. A., and Peters, J. S. (1993) *Plant Physiol. 102*, 261−267.
96. Fuks, B., and Homblé, D. J. (1999) *Biochim. Biophys. Acta 1416*, 361−369.
97. Bölter, B., Soll, J., Hill, K., Hemmler, R., and Wagner, R. (1999) *EMBO J. 18*, 5505−5516.
98. Pohlmeyer, K., Soll, J., Grimm, R., Hill, K., and Wagner, R. (1998) *Plant Cell 10*, 1207−1216.
99. van den Wijngaard, P. W. J., and Vredenberg, W. J. (1997) *J. Biol. Chem. 272*, 29430−29433.
100. Robinson, S. P. (1985) *Biochim. Biophys. Acta 806*, 187−194.
101. Keegstra, K., Olsen, L. J., and Theg, S. M. (1989) *Annu. Rev. Plant Physiol. Plant Mol. Biol. 40*, 471−501.
102. Werdan, K., and Heldt, H. W. (1975) *Biochim. Biophys. Acta 396*, 276−292.
103. Heber, U., and Heldt, H. W. (1981) *Annu. Rev. Plant Physiol. 32*, 139−168.
104. Heber, U. (1974) *Annu. Rev. Plant Physiol. 25*, 393−421.
105. Nobel, P. (1968) *Biochim. Biophys. Acta 153*, 170−182.
106. Debus, R. (1992) *Biochim. Biophys. Acta 1102*, 269−352.
107. Allakhverdiev, S. I., Sakamoto, A., Nishiyama, Y., Inaba, M., and Murat, N. (2000) *Plant Physiol. 123*, 1047−1056.
108. Cruz, J. A., Salbilla, B., Kanazawa, A., and Kramer, D. M. (2000) *Plant Physiol.* (submitted for publication).

BI0018741